Published in
Journal of Physics B: Atomic, Molecular and Optical Physics 28, issue 15, 3213-3224, 1995
which should be used for any reference to this work

The capture process in spherical magneto-optical traps: experiment and 1D magnetic field models

N Sagna, G Dudle and P Thomann

Observatoire Cantonal, Rue de l'Observatoire 58, CH-2000 Neuchâtel, Switzerland

Abstract. The influence of the magnetic field gradient on the number of Cs atoms captured in a three-dimensional magneto-optical trap is investigated both theoretically and experimentally. Two one-dimensional models of the capture process are proposed, which differ only by the nature of the assumptions on the effect of Zeeman optical pumping. Transverse cooling beams are accounted for by a mere modification of the scattering rate. Comparison with experiment shows that the number of trapped atoms versus laser detuning, laser intensity, laser beam diameter and magnetic field gradient is best predicted by a model including all Zeeman substates of the Cs atoms. Quantitative agreement is within a factor of three in most cases of interest.

1. Introdution

Since the first observation of magneto-optically trapped atoms [1], much progress has been made in the field of laser cooling on both the experimental and theoretical side. The fact that atoms can be slowed down directly from a thermal vapour rather than from a precooled atomic beam [2] has considerably simplified the experimental apparatus needed to produce cold atoms. This has opened up exciting perspectives in different fields of physics such as atomic optics [3], Bose–Einstein condensation, high-resolution spectroscopy [4] or frequency standards [5]. The three-dimensional situation makes a complete theoretical description too complicated to be solved analytically. Even with a numerical approach one needs to reduce the complexity of the problem. But, as will be shown, it is, however, possible to describe the general behaviour of a magneto-optical trap in a satisfactory manner with a 1D model including some essential 3D features. The goal of our work is the realization of an atomic clock using cold caesium atoms. In such a clock the number of atoms contributing to the signal strongly depends on the efficiency of the capture process of the magneto-optical trap (MOT). This paper presents measurements of the number of trapped atoms as function of the essential trapping parameters such as laser intensity, detuning or diameter. We also investigate the evolution of the number of atoms with the magnetic gradient. The results are compared with the predictions of a theoretical model. The paper is constructed as follows. Section 2 is the theoretical part where the basic ideas leading to two entirely one-dimensional models are developed. In section 3 the experimental set-up is explained in some detail; in section 4 the experimental data are discussed and compared with the theoretical predictions.

2. Theoretical models

In this section, two entirely one-dimensional models are presented. They describe the capture process and give predictions about the number of trapped atoms. While analytical treatments [2, 6] of the capture process and the number of atoms neglect the effect of the magnetic field, there is some experimental evidence [7] of the critical role that the magnetic field gradient plays in the capture process. To point out such a role, Lindquist *et al* [7] use a quasi-one-dimensional model that explicitly takes into account the three-dimensional nature of the magnetic field: the change in direction of the magnetic field is considered by averaging the cooling process over the cross section of the beam. In the following, we show that a simple one-dimensional model considering only a longitudinal magnetic field can satisfactorily describe the main features of the capture over a wide range of the magnetic gradient.

Both models presented here use a simple numerical simulation in order to take into account the magnetic field. They are different in the type of optical transition each of them considers but otherwise they are based on the same set of assumptions: we assume that the atoms move on the x-axis in a magnetic field $\boldsymbol{B}(x) = bx\boldsymbol{e}_x$ and are subjected to the radiation pressure of two counter-propagating, circularly polarized ($\sigma^{\pm}$) laser beams, with a wavevector $\boldsymbol{k} = \pm k\boldsymbol{e}_x$. One important feature of this description is that it only considers the magnetic field along the central axis of the beams where it is parallel to the wavevector. One is aware that this is unlike the real physical situation where most atoms experience a magnetic field that changes in direction. As described by Monroe *et al* [2] we further assume that the capture process is isotropic in a three-dimensional magneto-optical trap: when an atom enters the trapping volume, it sees a pair of co- and counter-propagating beams. Under these assumptions the capture process can be described by a one-dimensional model. Although most of the atoms enter the trap off-axis, the comparison of the predictions of the model with the experimental results shows that for small magnetic field gradients b and small beam diameter d such that $bd \leqslant 15$ G, the capture process as well as the influence of the magnetic field on it may be described by considering the on-axis case.

The equation of evolution of the number of atoms in a magneto-optical trap is given by [8]:

$$\frac{\mathrm{d}N}{\mathrm{d}t} = R - \frac{N}{\tau_{trap}} \tag{1}$$

where R is the trap capture rate and $1/\tau_{trap} = 1/\tau_{Cs} + 1/\tau_{Bg}$ is the loss rate due to collisions between the cold caesium atoms and atoms of the background (Cs and non-Cs) at thermal velocity. Intratrap collisions that generate nonlinear terms in the rate equation (1) are ignored. Their contribution is indeed negligible [9] for the densities (10^{11} cm^{-3}) we obtained. The trap loss rate is given by

$$\frac{1}{\tau_{trap}} = (n_0\sigma_{Cs}\overline{v}_{Cs}) + \left(\sum_i n_i\sigma_i\overline{v}_i\right) \tag{2}$$

where n_0 is the number density of the caesium background gas and $\sigma_{Cs} = 2 \times 10^{-13}$ cm^2 is the collision cross section between caesium atoms [10], $\overline{v}_{Cs}$ and $\overline{v}_i$ are the mean velocities of the thermal caesium background atoms and of the component i of the residual gas atoms relative to cold caesium atoms, respectively; since the cold atoms are approximately at rest, $\overline{v}_{Cs}$ and $\overline{v}_i$ are the mean velocities of the background atoms [11]. The capture rate R can be written as the number of atoms entering the trapping region—a sphere with diameter

d—per unit time, multiplied by that fraction of the atomic velocity distribution that lies below the capture velocity v_c of the trap [2]:

$$R = \frac{4}{\pi^2} n_0 S \frac{v_c^4}{v_{th}^3} \tag{3}$$

where $S = \pi d^2$ is the surface area of the trap volume, and

$$v_{th} = \sqrt{\frac{8}{\pi} \frac{k_B T}{m_{Cs}}}$$

is the mean velocity of the background caesium atoms. The steady-state number of trapped atoms is $N_S = R\tau_{trap}$; to determine N_S, one has to compute the capture velocity v_c. This is done by numerically determining the atomic trajectories by solving the Newtonian equation $m\dot{v} = F(x, v)$ where F is the force on an atom induced by the combined action of the light and the magnetic field gradient.

Derivation of the magneto-optical force

This force is supposed to be a Doppler-type one: it corresponds to the difference of radiation pressures of the two beams, due to both Doppler and Zeeman shifts. The models neglect the interferences between the two beams and the sub-Doppler processes they induce. The assumption of neglecting these processes is justified because sub-Doppler cooling and trapping that explain inner features of the trap, like its low-temperature and small size [11], can only occur for atomic velocities such that $kv \sim \Gamma_p$ where Γ_p is the optical pumping time [12]. This velocity condition is only fulfilled by atoms that are at the end of the capture process. Besides, one considers the average of the light pressure force on an atom over several fluorescence cycles of absorption and spontaneous emission of a photon. In the models presented here, we start from the average force F exerted on a two-level atom by a single monochromatic light beam:

$$F(x, v) = \hbar k \Gamma \frac{\beta(x)}{1 + 2\beta(x) + 4\delta_{eff}^2(x, v)} \tag{4}$$

where $\Gamma = 2\pi \times 5.3$ MHz is the natural decay rate of the caesium excited state, $\beta = I/I_{sat}$ is the saturation parameter of each beam and $I_{sat} = 2.2$ mW cm^{-2} is the intensity for which the Rabi angular frequency is equal to Γ for the $|F = 4, m_g = 4) \rightarrow |F' = 5, m_e = 5)$ transition; δ_{eff} is the effective detuning normalized to the decay rate Γ, that can include the laser detuning $\Delta = \omega_{laser} - \omega_{atom}$ and Zeeman and Doppler shifts. The linearized expression of the force ($F = -\alpha v + \kappa x$) commonly used [1] cannot be considered in describing the capture process: the magneto-optical force has a linear dependence on the position x and the velocity v only if $kv \ll \Gamma$, and $\mu_B b x \ll \hbar\Gamma$ and in most traps these conditions are only valid for already trapped atoms [11].

Despite their one-dimensional nature, both models presented here take into account the power broadening due to the three pairs of beams. In order not to overestimate the power broadening due to the transverse beams, one has to consider their Gaussian profile and therefore write the intensity term in the denominator of (4):

$$2\beta\left(2 + 4\exp\left(-2\left(\frac{x}{L/2}\right)^2\right)\right)$$

where the first term of the sum is related to the longitudinal beams while the second one describes the effect of the transverse beams. Indeed, we have found that a rectangular profile

for the transverse beams leads the model to underestimate the absorption rate of photons propagating along the x-axis and therefore the efficiency of the cooling in this direction. This is especially true for laser intensities such that $I/I_{sat} \geqslant 1$ and on the edge of the trap.

The expression of the force F depends on the transitions involved in the cooling process and that is where the two models differ. Knowing that under the action of the two circularly polarized beams, the atoms tend to be Zeeman pumped towards $m_F = \pm 4$, in the first model (three-level model) one exaggerates the effect of optical pumping by assuming that only the $m_F = \pm 4$ ground state sublevels are populated. This assumption, together with the consideration of the Clebsch–Gordan coefficients, allows one to reduce the $F = 4 \rightarrow F' = 5$ caesium transition to a $J = 0 \rightarrow 1$ transition. Since the sublevel $|J = 1, m_J = 0\rangle$ is decoupled, the atom reduces to a three-level system. The force can then be written as

$$F(x, v) = \hbar k \Gamma \beta \left[\frac{1}{1 + 4\beta\left(1 + 2\exp\left(-2\left(\frac{x}{L/2}\right)^2\right)\right) + 4\left(\frac{\Delta - (kv + \mu_B \hbar^{-1} bx)}{\Gamma}\right)^2} - \frac{1}{1 + 4\beta\left(1 + 2\exp\left(-2\left(\frac{x}{L/2}\right)^2\right)\right) + 4\left(\frac{\Delta + (kv + \mu_B \hbar^{-1} bx)}{\Gamma}\right)^2} \right]. \tag{5}$$

On the other hand, the second model (multi-level model) neglects the effect of optical pumping: all the ground state Zeeman sublevels are assumed to be equally populated. Such an assumption can be justified by the following two arguments. The first one is in line with the disregard of sub-Doppler processes: the σ^+–σ^- configuration leads to a total electric field with a linear polarization that rotates in space; for an atom moving with velocity v, the angular frequency of the polarization is given by [12] $\omega_{pol} = kv$. Moreover, for Cs atoms and our irradiation conditions, the Zeeman pumping time [13] is as long as $\tau_p \cong 3\ \mu$s. Therefore in the range of velocities important for the capture process (1–20 m s^{-1}) one has: $\omega_{pol}\tau_p \gg 1$; this means that population differences between ground state Zeeman sublevels do not have time to build up. The second argument relies on the fact that during the capture process, for most of the atoms the magnetic field changes in direction and magnitude and therefore tends to equalize the population of the Zeeman sublevels by Larmor precession. Indeed one sees that in the range of magnetic gradient used here, the Larmor frequency $\omega_L = \mu_B bx$ in the trapping region is such that $\omega_L \gg 1/\tau_p$, except inside the volume of the cold cloud where it becomes comparable in magnitude with $1/\tau_p$. Therefore we assume that the population of each Zeeman sublevel of the ground state is $\frac{1}{9}$ and we take into account all the $\Delta m = \pm 1$ transitions from the $F = 4$ ground state. The expression of the force is then given by

$$F(x, v) = \tfrac{1}{9}\hbar k \Gamma \sum_{m_g=-4}^{4} \left[\frac{\beta^+_{m_g}}{1 + 4\beta^+_{m_g}\left(1 + 2\exp\left(-2\left(\frac{x}{L/2}\right)^2\right)\right) + 4\delta^{+2}_{m_g}(x, v)} - \frac{\beta^-_{m_g}}{1 + 4\beta^-_{m_g}\left(1 + 2\exp\left(-2\left(\frac{x}{L/2}\right)^2\right)\right) + 4\delta^{-2}_{m_g}(x, v)} \right] \tag{6}$$

where $\beta^{\pm}_{m_g}$ is the saturation parameter associated to the transition $|F = 4, m_g\rangle \rightarrow |F' = 5, m_g \pm 1\rangle$; $\delta^{\pm}_{m_g}(x, v)$ is the corresponding effective detuning, normalized to Γ, and is given

by

$$\delta^{\pm}_{m_g}(x, v) = \frac{1}{\Gamma}\left(\Delta \mp kv - \frac{\mu_B b x}{\hbar}\left(\left(m_g \pm 1\right) g_e - m_g g_g\right)\right) \tag{7}$$

where $g_e = 0.4$ and $g_g = 0.25$ are the Landé g factors of the excited and ground levels, respectively. From expressions (5) and (6) one determines the capture velocity by solving the Newtonian equation and hence the number of trapped atoms predicted by the two models.

3. Experimental set-up

The two main parts of a MOT experiment are the laser light preparation and the magnetic gradient. In this section we describe the two parts as they are used in this study. In addition, a short description of the detection chain is given.

A well known way of producing a magnetic gradient is the anti-Helmholtz coil pair [1, 2, 7]: two coaxial loops of diameter $2r$ are placed in parallel planes separated by $2a$. The two loops are supplied with equal currents of opposite sign. The zero divergence of the magnetic field and the rotational symmetry imply $\mathrm{d}B_y/\mathrm{d}y = \mathrm{d}B_z/\mathrm{d}z = -0.5\mathrm{d}B_x/\mathrm{d}x$ if x is the common axis of the coils.

For this work a slightly different solution has been chosen (see figure 1). Four straight wire conductors parallel to the vertical z-axis with a length of 200 mm are placed on a square with a side of 66 mm centred at the origin. If adjacent conductors are supplied with currents of opposite sign this array produces a two-dimensional quadrupole field in the horizontal (xy)-plane. A second, independent set of conductors parallel to the y-axis, placed on a square with a side of 86 mm adds a similar quadrupole field in the (xz)-plane. The combination of both structures yields a gradient almost equivalent to that of the anti-Helmholtz coils.

This fact is not surprising since near the centre the eight conductors together form two rectangular quasi-loops parallel to the (yz)-plane with opposite currents in the two loops. If the x-axis is a rotational symmetry axis in the case of anti-Helmholtz coils, it is a four-fold axis here. Each four-wire structure can produce a maximum gradient $\mathrm{d}B_x/\mathrm{d}x$

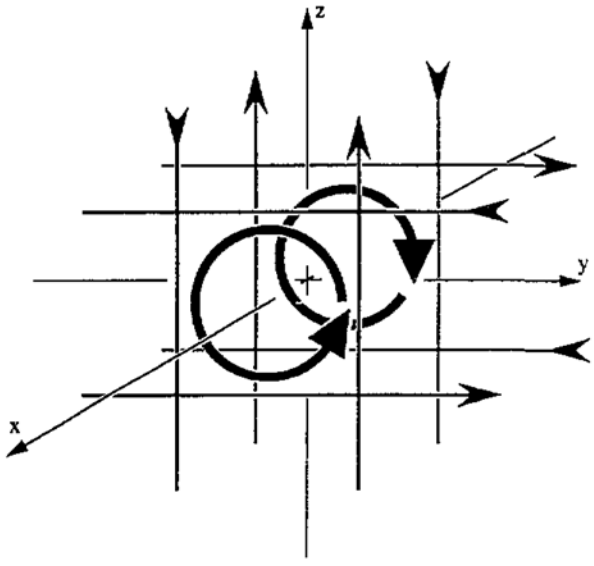

Figure 1. Scheme of the magnetic gradient. Four straight currents (length 200 mm) parallel to the z-axis placed on a square (side 66 mm) produce a quadrupole magnetic field in the (xy)-plane, and an analogous set of four currents parallel to the y-axis a similar field in the (xz)-plane. This results in a situation close to that of the anti-Helmholtz coils symbolized by the two circles.

of 7.5 G cm^{-1}. When both structures are operated at maximum current, the x-component reaches 15 G cm^{-1}. Due to the independence of the current segments, this assembly can be used not only to study three dimensional magneto-optical traps but also to investigate anisotropic situations of a 2D trap.

All lasers used in the experiment are diodes. Different constraints on the laser frequency, linewidth, polarization and intensity have to be fulfilled to slow down thermal atoms. The laser linewidth has to be narrower than the natural linewidth of the caesium D_2 transition ($\lambda = 852$ nm, $\Gamma = 2\pi \times 5.3$ MHz). Previous work [14] has shown that commercially available laser diodes are spectrally too broad to be used directly and must be line-narrowed. We place the diode treated with an AR coating on the output facet in an extended cavity closed by a diffraction grating at the Littrow angle [15] to reduce the linewidth below 1 MHz; the range over which the laser can be continuously tuned without cavity mode hops is about 10 GHz. About 25% of the output of the stand-alone laser diode is extracted from the extended cavity configuration.

This low power laser beam is divided into two parts: one is used to offset-lock the extended cavity laser to the transition $F = 4 \rightarrow F' = 5$ of the D_2 line of caesium resolved in a vapour cell by saturated absorption. The second part is used to control the output of a higher power (typically 50 mW) laser by injection locking. On both arms an acousto-optic modulator shifts the laser frequency by a controllable amount. The combined effect of the two modulators allows the high power laser to be tuned in a precisely controlled way around the 4–5 transition frequency. The tuning range is $\pm 5\Gamma$. After passing through a set of anamorphic prisms this slave laser beam is spatially filtered in a beam-expanding telescope. The output beam has a final circular $1/e^2$ diameter L of 14 mm. At this stage a diaphragm controls the diameter of the cooling beams: even at the smallest diameter (3 mm), diffraction effects from the diaphragm placed 3 m away from the trap were found to be negligible. We used this diaphragm to study the dependence of the number of atoms on the beam diameter. This means that the $1/e^2$ diameter of the Gaussian-shaped beam stays unchanged, only its wings are truncated at a given diameter d. The beam is then divided into five parts. Four of them are used to produce two standing waves in a vertical (yz)-plane, the fifth one propagates along the horizontal x-axis, which is also the common axis of the rectangular loops, and forms a standing wave by retroreflection. The beams in the (yz)-plane are at an angle of 45° to the horizontal plane, such that no beam propagates parallel to the vertical axis (z). Before penetrating the vacuum chamber the circular polarization needed for the operation of the MOT [1] is given to each beam by $\lambda/4$ retarder plates. All beams enter parallel to each other, through the same window, into the vacuum chamber and are redirected inside by 45° mirrors towards the trap centre. The light of an additional laser is mixed to one of the cooling beams after the telescope. This laser, locked to the transition $F = 3 \rightarrow F' = 4$ using a Doppler-free saturated absorption cell, prevents atoms from accumulating in the state $F = 3$ which is decoupled from the cooling beams. This repumping beam is provided by a DBR diode laser with 3 mW output and has an approximate linewidth of 5 MHz.

The stainless steel vacuum vessel contains the two sets of four straight wire conductors to form the magnetic gradients and four 45° mirrors. The whole volume of the chamber is filled with caesium vapour; its density can be controlled by varying the temperature of a finger with an initial 1 g load of caesium. Light absorption across the chamber can be used to measure the Cs density. The residual pressure is less than 10^{-8} mbar.

For the visualization as well as for the different measurements performed on the cold atoms, a CCD camera has been installed. The camera is connected to a personal computer with image processing software. This allows the direct integration of the radiated power

over the surface of the image produced by the cloud. Care has been taken to correct for the non-linear response of the CCD. With that detection chain the light radiated by the trapped atoms is easily measured. If the cloud of atoms is optically thin, the total power can be deduced by taking into account the solid angle of the collection optics. Knowing the scattering rate one can deduce the total number of atoms from the fluorescence power.

4. Results and discussion

We start with three preliminary remarks related to the numerical values of the intensity and the magnetic gradient used in the theoretical models. As mentioned in section 3, the x-component of the gradient is twice as large as the other components. The theoretical models are unidimensional and can therefore not handle anisotropic gradients. To be closer to physical reality we use $\frac{2}{3}$ of the x-component as an average value of the gradient in our calculations. This is clearly an approximation since the dependence of the number of trapped atoms on the magnetic gradient is neither linear nor weak (figure 6). Another important parameter is the intensity. We want the atoms entering the trap on-axis to be representative of the capture process. Due to the Gaussian profile of the beam, atoms moving far from the x-axis are subjected to a lower intensity than those closer to the axis. We account for that by using an average intensity in the calculations. This average intensity corresponds to the power within the $1/e^2$ diameter L divided by the corresponding surface $L^2\pi/4$. Values of the intensity in the figures below refer to this average intensity. Let us finally point out that in order to facilitate the comparison between the experimental and the theoretical behaviour, the numerical predictions have, in all cases, been multiplied by a normalization factor. The aim of our models is not to reproduce the absolute number of cold caesium atoms in a cloud. Even if a full 3D quantum mechanical model of a trap were to be developed, the imperfections in the trapping conditions (misalignment and

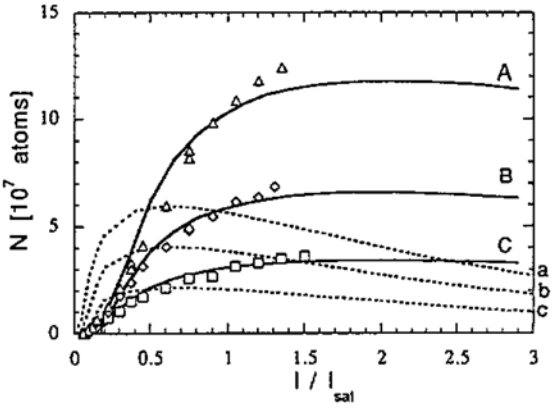

Figure 2. Number of trapped atoms versus cooling beam intensity for three magnetic gradients. The $1/e^2$ diameter of the cooling beams is 14 mm. The symbols represent the experimental data whereas the lines are the predictions of the theoretical model multiplied by a normalization factor. Full curves designated by upper case letters are the curves of the multi-level model, dotted lines with lower case letters those of the three level model. The detuning has been optimized for each curve. See table 1 for the key to the figure.

Table 1. Key to figure 2.

	A(a)	B(b)	C(c)
Experimental values	Δ	◊	□
dB_x/dx (G cm^{-1})	12	6	4
Detuning (Γ)	−2	−1.7	−1.3
Normalization factor	3.81 (1.1)	2.4 (0.78)	1.35 (0.44)

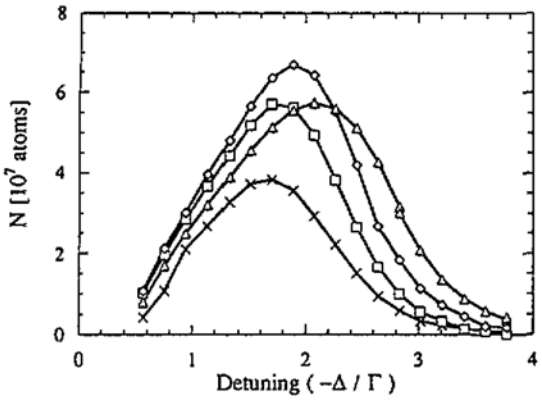

Figure 3. Number of trapped atoms as a function of laser detuning for different values of the magnetic gradient. The $1/e^2$ diameter of the cooling beams is 14 mm. Experimental points are joined by lines for clarity. (△) dB/dx = 14 G cm^{-1}, (◇) 10 G cm^{-1}, (□) 8 G cm^{-1} and (×) 6 G cm^{-1} and constant laser intensity ($1.8I_{sat}$ per beam).

intensity imbalance of the laser beams, spurious magnetic field), as well as uncertainties in the detection chain (calibration, optical thickness of the cold cloud) would make it very difficult to predict absolute numbers of trapped atoms. Rather one investigates the ability of the models to describe the dependence of the number of trapped atoms on the trapping parameters. One therefore uses different normalization factors for each experimental curve.

Figure 2 shows the dependence of the number of trapped atoms on the cooling laser intensity for different values of the magnetic gradient. The values on the abscissa correspond to the average intensity of each of the six cooling beams and are normalized to the saturation intensity of the transition $|F = 4, m_g = +4\rangle \rightarrow |F' = 5, m_e = +5\rangle$ as defined above. In the same graph we represent the predictions of the multi-level (full curves) and the three-level model (dotted curve). As will be shown later, the detuning that maximizes the number of trapped atoms depends on the magnetic gradient. For each of the three data sets in figure 2 we have therefore used the optimum detuning. Apparently the three-level model fails in accurately describing how the capture process depends on laser intensity and magnetic field: indeed, as shown in figure 2, it predicts that as the laser intensity increases the number of trapped atoms reaches a maximum (around I_{sat}) and then tends to a lower value. Such a pronounced behaviour has not been observed experimentally. The multi-level model, on the other hand, exhibits a much smoother maximum of trapped atoms. This maximum number is reached at a higher intensity and decreases only by a small amount beyond this optimum value. Although the available laser power did not allow us to investigate this saturation phenomena the behaviour at low laser intensity is in better agreement with the multi-level model.

Figure 3 shows the number of trapped atoms as a function of the cooling laser detuning. Two important features have to be emphasized in this graph. First, as already mentioned, the optimum detuning increases with the magnetic gradient, as expected. Secondly the maximum number of trapped atoms goes through a maximum as the magnetic gradient is increased. This behaviour is also predicted by the theory although the agreement between experimental and theoretical data is not perfect as can be seen in figure 6. All the optimum detunings observed experimentally lie between -1.6Γ and -2.2Γ. Our numerical simulations have shown that the dependence of the optimum detuning on the magnetic gradient predicted by the two models is not as strong as the one measured: for magnetic gradient values ranging between 4 and 15 G cm^{-1}, the multi-level (three-level) model predicts values between -1.6Γ and -1.8Γ (-1.8Γ and -2Γ)

A direct comparison between the predictions of the two models in figure 4 does not give a clear preference for one of the two models: considering the approximations made in

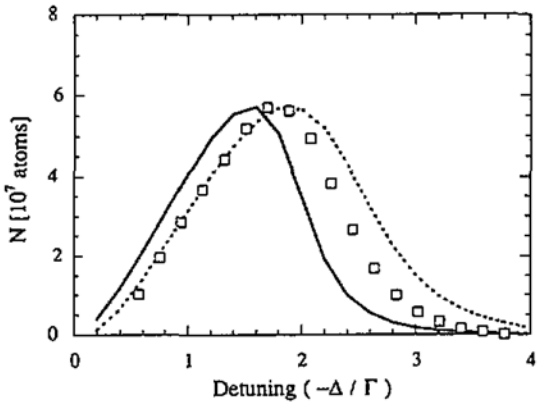

Figure 4. Comparison between the predictions of the three-level model and the multi-level model concerning the number of trapped atoms as a function of laser detuning. The $1/e^2$ diameter of the cooling beams is 14 mm. The symbols (□) represent the experimental values obtained with a magnetic gradient of $dB/dx = 8$ G cm^{-1} and a laser intensity of 1.8 I_{sat} per beam. The full curve refers to the multi-level model, the dotted curve to the three-level model. To fit the experimental values both curves have been multiplied with a normalization factor (2.0 for the multi-level, 1.16 for the three-level model)

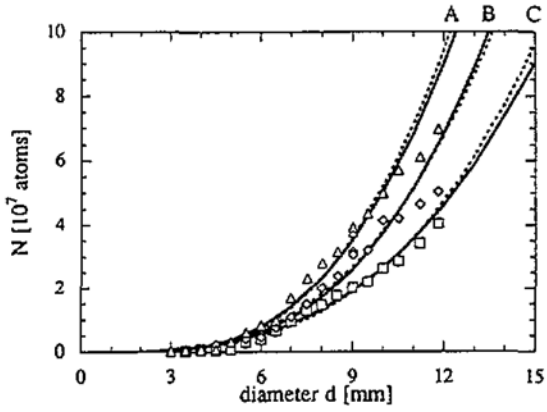

Figure 5. Number of trapped atoms versus beam diameter. The $1/e^2$ diameter of the beam is 14 mm for all the experimental data. The values on the abscissa refer to the diameter d at which the Gaussian shaped beams have been truncated. The three series of measurements correspond to different values of the magnetic gradient. See table 2 for the key to the figure.

Table 2. Key to figure 5.

	A(a)	B(b)	C(c)
Experimental values	Δ	◊	□
dB_x/dx (G cm^{-1})	12	6	4
Normalization factor	1.67 (0.98)	1.45 (0.85)	0.82 (0.65)

the model, the fact that the normalization factor of the multi-level model is larger (2.0 for multi-level, 1.16 for three-level model) cannot be considered as conclusive.

The capture velocity and hence the number of trapped atoms depends strongly on the beam diameter. To investigate the law connecting the number of atoms and the beam diameter, the Gaussian profile of the beam is truncated by a diaphragm placed at the output of the telescope. Figure 5 shows the experimental curves corresponding to three different values of magnetic gradient. In all three cases the agreement between theory and experiment is reasonably good for diameters in the range between 3 and 12 mm and there is no significant difference between the predictions of the two models.

The three-level model is the simplest that takes into account the magnetic field. Its predictions reproduce, as shown in figures 3 and 5, the general behaviour of the number of atoms as a function of parameters such as the laser detuning and the beam diameter. Despite its simplicity it predicts the number of trapped atoms with good accuracy with normalization factors lying between 0.7 and 1.2. However, this model fails in describing how the capture

process depends on the laser intensity and the magnetic field gradient. This failure shows that the assumption of optical Zeeman pumping towards $m_F = \pm 4$, which only retains the transition with the smallest saturation intensity, tends to overestimate the effect of power broadening. This is the only point on which the two models exhibit a clear difference in their predictions. Figure 2 shows that an accurate description of the saturation effects requires the consideration of all Zeeman sublevels. Despite the necessity to normalize its prediction by a factor varying between 1 and 3.1, the multi-level model accurately reproduces (figure 2) how the number of trapped atoms depends on the laser beam intensity. This good agreement underlines the fact that the model closely matches the real physical situation: although one regards the cooling and the trapping in only one direction, the scattering rate of the atoms is power broadened by the combined effect of the three pairs of beams. We have tested the importance of the six-beam power broadening in the model by only considering the effect of one (like in [7]) and two beams: we found that the experimental dependences on intensity and diameter are no longer reproduced, especially for saturating intensities. As shown in figures 2–5 the predictions of the multi-level model match the experimental data for magnetic field gradients between 4 and 12 G cm^{-1}. For larger values of the gradient the model still predicts most of the general behaviour; however, we found that the normalization factor tends to increase up to 3.1 and the difference between the experimental and predicted optimum detuning rises to 0.5 Γ for a gradient of 15 G cm^{-1}.

The good agreement of the multi-level model with the experimental data justifies *a posteriori* the use of an entirely one-dimensional model to describe the trapping process in the MOT with $bd \leqslant 15$ G. Such a situation, in which the atoms entering the trap on-axis are representative of the general capture process, is in contrast to that analysed by Lindquist [7]. In addition, our description requires a simpler numerical computation than that of [7] since it avoids the averaging of the capture velocity over the beam intersection. This shows that a three-dimensional MOT can be described by a purely one-dimensional model provided that some consequences of 3D features, such as the power broadening of the transverse beams and the mixing of the Zeeman sublevel populations by the 3D changing magnetic field, are properly taken into account.

Moreover, the experimental results and the theoretical dependences of the number of trapped atoms on the magnetic field gradient emphasize the role of the magnetic field in the capture process and the limits of a one-dimensional model. As shown in figure 6, for given laser detuning, intensity, and beam diameter, there is a magnetic field gradient that optimizes the number of trapped atoms. Both models predict the existence of this optimum gradient but they fail in predicting its value to better than $\pm$ 3 G cm^{-1}. In addition to that, one also

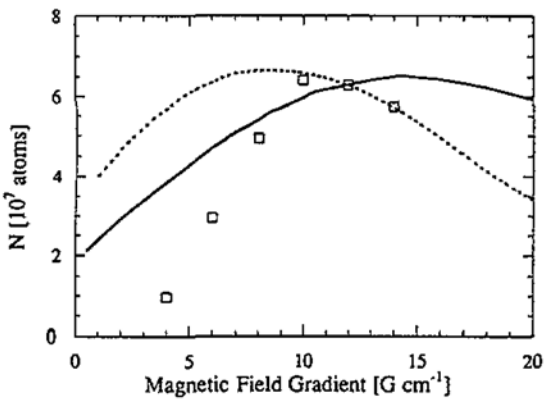

Figure 6. Number of trapped atoms versus the x component of the magnetic gradient ($dB/dy = dB/dz = 0.5dB/dx$). The $1/e^2$ diameter of the cooling beams is 14 mm. The laser detuning and intensity are kept constant ($\Delta = -2\Gamma$, $I = 1.8I_{sat}$). The symbols (□) are experimental values, the full (dotted) curve represents the theoretical prediction of the multilevel (three-level) model.

notices a serious discrepancy between the predicted and the measured number of trapped atoms for low magnetic field gradients. In fact, the two models reproduce the general behaviour of the experimental data but they do not predict an optimum number of trapped atoms as pronounced as the one measured. This can be explained by the fact that the one-dimensional models only consider the effects of the on-axis magnetic field and therefore only regard a partial influence of the 3D magnetic field. The existence of an optimum magnetic gradient in the one-dimensional description suggests that the longitudinal magnetic field influences the capture process in two different ways whose relative importance varies with the gradient. For low values of the gradient, the predominant contribution arises from the fact that the magnetic field tends to curve the atomic trajectories in the (x, v) phase diagram. As the magnetic gradient increases, the first turning point (where the atomic velocity vanishes) is drawn nearer to the centre, thereby increasing the capture velocity [16]. This effect of the magnetic field ceases to be dominant when the Zeeman shifts at the edge of the trapping region are no longer negligible compared to the laser detuning and the Doppler shifts; the longitudinal magnetic field then perturbs the slowing process by reducing the friction coefficient [17]. Therefore at large values of the gradient, the capture velocity and hence the number of trapped atoms decreases with the gradient.

One might also invoke the unavoidable fact that one-dimensional models neglect some effects of the transverse components of the magnetic field on the capture process: we have included a tranverse field in the computation of the average Doppler force and we have indeed noticed that it tends to reduce the friction coefficient in a non-negligible way. However, the predicted influence of the magnetic field strength on the number of trapped atoms does not differ appreciably from that of more elaborate models that include transverse fields [7]. The difference between the predictions of the 1D models and the experimental results at low magnetic gradient could also be partly explained by the fact that our models disregard loss phenomena other than collisions between hot and cold caesium atoms. At low magnetic gradient the trap becomes very sensitive to imperfections in the alignment or in the intensity balance that lead to spatial diffusion and atomic drift.

5. Conclusion

We underline the role of the different parameters of a magneto-optical trap using two simple one-dimensional models that take into account the magnetic field gradient and the power broadening due to the transverse beams. With the predictions of the models, we point out how to optimize the number of trapped atoms. It is shown that the most accurate predictions are given by the model that takes into account a typical feature of a 3D magneto-optical trap: the mixing of the population of the Zeeman sublevels by the magnetic field that counteracts optical pumping. For the description of the capture process, the essential consequence of the 3D nature of the magnetic field, is that the Zeeman sublevel populations are equalized. This feature allows a greatly simplified, but still realistic, description of the capture process which is purely one-dimensional. It is also demonstrated that the magnetic field influences the capture process by both bending the trajectories and reducing the friction coefficient when the Zeeman shifts are important enough to perturb the cooling.

Acknowledgments

The authors wish to thank A Clairon for the many helpful discussions and advice. This work was supported by the Swiss National Science Foundation and the Swiss Federal Office of Metrology.

References

[1] Raab E L *et al* 1987 *Phys. Rev. Lett.* **59** 2631
[2] Monroe C, Swann W, Robinson H and Wieman C 1990 *Phys. Rev. Lett.* **65** 1571
[3] Aminoff C G *et al* 1993 *Phys. Rev. Lett.* **71** 3083
[4] Grison D *et al* 1991 *Europhys. Lett.* **15** 149
[5] Santarelli G *et al* 1994 *Proc. 8th European Frequency and Time Forum (München)* vol 1 FSRM, Swiss Foundation for Research in Microtechnology, Rue de l'Orangerie 8, CH 2000 Neuchâtel, Switzerland pp 46–57
[6] Gibble K, Kasapi S and Chu S 1992 *Opt. Lett.* **17** 526
[7] Lindquist K, Stephens M and Wieman C E 1992 *Phys. Rev.* A **46** 4082
[8] Sesko D W, Walker T G and Wieman C E 1991 *J. Opt. Soc. Am.* B **8** 946
[9] Sesko D W *et al* 1989 *Phys. Rev. Lett.* **63** 961
[10] Esterman I, Foner S N and Stern O 1947 *Phys. Rev.* **71** 250
[11] Steane A, Chowdhury M and Foot C 1992 *J. Opt. Soc. Am.* B **9** 2142
[12] Dalibard J and Cohen-Tannoudji C 1989 *J. Opt. Soc. Am.* B **6** 2023
[13] Thomann P and Hadorn F 1989 *Proc. 3rd European Frequency and Time Forum (Besançon)* FSRM, Swiss Foundation for Research in Microtechnology, Rue de l'Orangerie 8, CH 2000 Neuchâtel, Switzerland pp 269–73
[14] Sagna N, Mandache C and Thomann P 1992 *Proc. 6th European Frequency and Time Forum (Noordwijk)* ed J J Hunt (Noordwijk: ESA Publication Division) pp 521–5
[15] Sampei S *et al* 1983 *Japan. J. Appl. Phys.* **22** 258
[16] Grison D 1992 *PhD Thesis* Université Paris VI
[17] Walhout M, Dalibard J, Rolston S L and Phillips W D 1992 *J. Opt. Soc. Am.* B **9** 1997